NACA

RESEARCH MEMORANDUM

EFFECT OF FLIGHT SPEED ON DYNAMICS OF A TURBOPROP ENGINE

By S. Nakanishi, R. T. Craig, and D. B. Wile

Lewis Flight Propulsion Laboratory
Cleveland, Ohio

NATIONAL ADVISORY COMMITTEE
FOR AERONAUTICS
WASHINGTON

April 11, 1955
Declassified February 8, 1957

NATIONAL ADVISORY COMMITTEE FOR AERONAUTICS

RESEARCH MEMORANDUM

EFFECT OF FLIGHT SPEED ON DYNAMICS OF A TURBOPROP ENGINE

By S. Nakanishi, R. T. Craig, and D. B. Wile

SUMMARY

Transient operation of a turboprop engine was investigated in an altitude wind tunnel at a simulated altitude of 35,000 feet over a range of Mach numbers from 0.15 to 0.5 to determine the effect of flight speed upon the dynamic response of the engine. The step-input technique was used to obtain the response of engine rotational speed to propeller-blade-angle and fuel-flow distrubances. Values of time constant calculated from steady-state data are compared with results obtained from harmonic and semilog analyses.

The generalized time constant of the engine-propeller combination varied with flight speed and power level. The steady-state performance characteristics of the propeller and engine were utilized to predict the time constant at various flight speeds, and the calculated value agreed with the time constant experimentally obtained from blade-angle transients. For both the blade-angle and fuel-flow inputs, the value of the time constant was invariant with direction and size of disturbance to ±10 percent speed changes.

INTRODUCTION

In the design and analysis of an automatic control system for a gas-turbine engine, knowledge of the transient performance characteristics of the engine, together with a practical method of expressing these characteristics, is desirable. As an initial step toward this end, a mathematical expression of the transient relation between various input and output engine variables at a given operating condition may be formulated. Understanding the transient engine behavior over a broad range of engine operating conditions then requires a knowledge of the variations in the coefficients of the basic mathematical expression caused by varying flight conditions or power settings. Although experimental transient investigation of a given engine directly renders the transient performance characteristics at the conditions investigated, a reliable method of predicting the transient performance of any engine at any flight condition by calculation from steady-state performance maps is a highly useful tool in control synthesis and design.

From previous investigations on turboprop engines (refs. 1 to 3), the transient response was found to be first order and linear for ±10-percent change in speed over the entire operating speed range. In reference 1 the time constant of the engine-propeller combination calculated from steady-state performance characteristics was found to agree very well with the time constant obtained experimentally. Furthermore, the generalized values of time constant were invariant over a range of pressure altitudes. The static sea-level investigation of reference 3 indicates agreement between calculated and experimental time constants within 14 percent. Because both investigations were conducted at constant flight speeds, the effects of flight speed on transient performance were not determined. The purpose of the work reported herein was to develop a method of facilitating the prediction of engine response time in order to study the effects of flight speed on the dynamics of a turboprop engine. In addition, information on the degree of reliability of such a method of calculation was desired.

In order to achieve these objectives, experimental studies were made of the response of engine rotational speed to fuel-flow and propeller-blade-angle disturbances. The investigation covered transient performance at a simulated altitude of 35,000 feet over a range of flight Mach numbers from nominal values of 0.15 to 0.5. By utilizing the steady-state characteristics and the calculation method presented herein, the variations in transient performance with flight speed were predicted. Relative effects of propeller and engine upon the transient performance at various flight speeds were studied. The extent to which the engine held to a linear first-order response as well as to the quasi-static assumptions on which the calculation method is based was then determined by comparison of the calculated and experimentally obtained time constants.

Because of the different manner in which flight speed affects the propeller and the engine, the dynamic characteristics of a turboprop engine cannot be expected to generalize. However, standard generalized forms are used to present all results on a comparable basis.

ANALYSIS

The exact mathematical description of the dynamics of a gas-turbine engine leads to equations whose solutions are extremely difficult to obtain. The general approach, therefore, is the representation of the system dynamics by linearized differential equations for excursions of limited size about a steady-state operating point. Equations thus obtained are more readily solved so that the response of rotational speed, say, of a turboprop engine to a finite disturbance in propeller blade angle can be amply described.

The solution of a differential equation that describes the transient response of a first-order linear system is characterized by a system time constant. The analytical determination of the time constant is accomplished by substituting proper coefficients into the equation defining the time constant. These coefficients or gains are a measure of the engine's sensitivity of one variable in response to another variable. The quasi-static assumptions of a linearized dynamic analysis state that these gains can be obtained from the slope, at a given operating point, of a steady-state performance curve of the one variable plotted as a function of the other.

The prediction of time constant over a range of flight speeds thus requires a steady-state performance map of the desired variables at each flight speed. In the event that such maps are unavailable for all the conditions desired, a generalization and extrapolation technique or some other method must be utilized to obtain the necessary information.

The following analysis is devoted to a consideration of the turboprop-engine variables pertinent to calculation of the time constant. A method is also developed whereby the prediction of the time constant in the absence of sufficient steady-state performance data can be accomplished.

Previous work on turboprop engines indicates that at a given flight condition the response of engine speed to fuel flow at a constant blade angle is

$$\left(\frac{\Delta N_e}{\Delta W}\right)_\beta = \frac{\left(\frac{\partial Q}{\partial W}\right)_{N_e}}{\left(-\frac{\partial Q}{\partial N_e}\right)_W + \left(\frac{\partial Q}{\partial N_e}\right)_\beta + (I_e + I_p')S} \tag{1}$$

where S is the Laplace operator and denotes the derivative $\frac{d}{dt}$.

Suitable use of gear ratios permits the use of engine shaft speed in this equation. The definitions of symbols used throughout the report are given in appendix A.

Similarly, the response of engine speed to blade angle at constant fuel flow is

$$\left(\frac{\Delta N_e}{\Delta \beta}\right)_W = \frac{\left(\frac{\partial Q}{\partial \beta}\right)_{N_e}}{\left(-\frac{\partial Q}{\partial N_e}\right)_W + \left(\frac{\partial Q}{\partial N_e}\right)_\beta + (I_e + I_p')S} \tag{2}$$

Both responses have the same associated time constant, namely,

$$\tau = \frac{I_e + I_p'}{\left(-\dfrac{\partial Q}{\partial N_e}\right)_W + \left(\dfrac{\partial Q}{\partial N_e}\right)_\beta} \tag{3}$$

The partial derivative $\left(\dfrac{\partial Q}{\partial N_e}\right)_W$, also called the torque-speed gain at constant fuel flow, can be readily evaluated as the slope of a curve defining torque as a function of engine speed during constant fuel-flow operation. In like manner, the torque-speed gain at constant blade angle $\left(\dfrac{\partial Q}{\partial N_e}\right)_\beta$ can be evaluated from operation at a constant propeller blade angle. In this manner, equation (3) was used in obtaining the calculated time constant. Full development of the preceding equations is given in reference 1.

Propeller Dynamics

In the analysis of propeller dynamics, the propeller torque at constant altitude and ram pressure is generally considered to be a function of blade angle and speed:

$$Q_p = f(N_p, \beta) \tag{4}$$

It is found in reference 1 that at different altitudes the blade angles and steady-state torques identified with a given corrected engine speed and corrected tail-pipe temperature were not identical. The slopes of the generalized torque-speed curves $\left(\dfrac{\partial Q}{\partial N_e}\right)_\beta \dfrac{\sqrt{\theta}}{\delta}$ at a given engine speed, however, were found to be practically independent of altitude. The dynamic response of the propeller, therefore, could be generalized for a range of altitudes, even though the steady-state performance did not completely generalize.

As the propeller is operated at different flight speeds, the values of propeller blade angles used in maintaining the engine speed and power within normal operating range will vary widely. Depending upon the characteristics of the propeller, the torque-speed function and hence $\left(\dfrac{\partial Q}{\partial N_e}\right)_\beta$ will normally vary in a manner much different from that found during altitude changes. To predict the propeller dynamics under such conditions requires a description of the propeller characteristics over the enter range of flight speeds encountered.

The variables affecting propeller performance can be grouped in dimensionless parameters. Two of these parameters, the power coefficient and the advance ratio, have a functional relation that forms a family of lines with a third parameter, the blade angle. From such a performance map, it is possible to determine the torque-speed characteristics at any specific flight condition by selecting the values of flight variables peculiar to that condition.

Assuming that the propeller power coefficient at a given propeller blade angle can be represented by a second-degree polynomial in $\frac{V}{N_p D_p}$, or advance ratio, gives

$$C = \frac{2\pi N_p Q_p}{\rho N_p^3 D_p^5} = a + b\left(\frac{V}{N_p D_p}\right) + c\left(\frac{V}{N_p D_p}\right)^2 \tag{5}$$

Referring the propeller torque to engine shaft speed, combining constants, and taking partial derivatives with respect to engine speed N_e give

$$\left(\frac{\partial Q_p'}{\partial N_e}\right)_{\beta, \rho, V} = \rho(2l N_e + mV) \tag{6}$$

By taking into account the gear-box losses, which are included in the torque measurement, the equation becomes

$$\left(\frac{\partial Q}{\partial N_e}\right)_\beta = (1 + h)\left(\frac{\partial Q_p'}{\partial N_e}\right)_\beta + \frac{2573.5}{N_e^2} \tag{7}$$

where $\left(\frac{\partial Q_p'}{\partial N_e}\right)_\beta$ is defined by equation (6). Detailed development of these equations is given in appendix B.

Engine Dynamics

In addition to the use of the propeller torque-speed information previously discussed, engine torque-speed information is needed for time-constant calculation. If available experimental data can be properly generalized, the torque-speed characteristics can be extrapolated for conditions of operation not covered by the experimental data.

Previous investigations on turbojet engines indicate that the basic gains of the engine itself can be generalized by use of standard parameters (refs. 4 and 5). The generalization of $\left(\frac{\partial Q}{\partial N_e}\right)_W$, which is an engine function, is therefore considered sufficiently correct over the range of subsonic flight Mach numbers covered in the present investigation.

In summary, the analytical determination of the time constant requires the evaluation of the two gains $\left(\dfrac{\partial Q}{\partial N_e}\right)_\beta$ and $\left(\dfrac{\partial Q}{\partial N_e}\right)_W$ at a steady-state operating point where the rotational speeds and the torques of the propeller and the engine are matched. At simulated flight conditions where the necessary steady-state experimental data are available, the torque-speed gains are readily evaluated from steady-state performance maps. For operating regions where experimental performance data are unavailable, torque-speed gains at constant blade angle, evaluated from the propeller characteristics curves, and extrapolated values of torque-speed gains at constant fuel flow are used to predict the time constant.

APPARATUS AND INSTRUMENTATION

Wind-Tunnel Installation

The turboprop engine was wing-mounted in the 20-foot-diameter test section of the NACA Lewis altitude wind tunnel as shown in figure 1(a). The tunnel had facilities for simulating flight conditions at a steady-state operating point by controlling air temperature, air speed, and altitude pressure. An exhaust-gas scoop located downstream of the engine removed hot exhaust gases from the tunnel stream.

Engine and Propeller

The turboprop engine had a nominal static sea-level rating of 2520 shaft horsepower and a jet thrust of 603 pounds at military operating conditions. A schematic drawing of the engine is shown in figure 1(b). The main components included a 19-stage axial-flow compressor, eight cylindrical can-type combustors, a four-stage turbine, and an exhaust cone. The engine was connected through a 12.5:1 reduction gear box to a 13-foot-diameter three-bladed propeller.

Input Systems

Input disturbances in fuel flow were imposed by a separate fast acting valve and regulator. Blade-angle disturbances were accomplished by a modified engine servo system.

Instrumentation

Instrumentation on the test installation was designed to measure and record transient data as well as steady-state data at the end points of the transient runs. The steady-state and transient instrumentation used

in the investigation are listed in table I. Proper design and fabrica-
tion techniques were incorporated to obtain the desired accuracy and
frequency-response characteristics. All transient data were recorded on
direct-inking strip-chart oscillographs with associated amplifiers for
each channel.

PROCEDURE

Desired flight conditions were simulated in the altitude wind tunnel
by setting the air temperature, tunnel air speed, and altitude pressure.
For transient runs involving fuel-flow disturbances, the propeller blade
angle was set at a given value and fuel flow was increased or decreased
in step sizes necessary to obtain the desired engine-speed change. Engine
power level was varied by setting different values of the blade angle.

Transient runs with blade-angle disturbances were made by maintaining
constant fuel flows of various magnitudes while the blade angle was in-
creased or decreased to obtain the desired terminal speeds.

Both types of input disturbances were made to cause increases and
decreases in the engine rotational speed. Steady-state data were taken
at the beginning and end of each transient after engine operating con-
ditions had reached equilibrium.

RESULTS AND DISCUSSION

The time constant characterizing the transient speed response of
the turboprop engine was calculated from equation (3) as set forth in
the ANALYSIS section. The steady-state experimental information used in
the development of the analytical method is presented herein followed
by a presentation of predicted time constant and a discussion of the
effects of flight speed upon the dynamics of the turboprop engine.

Time constant was also evaluated experimentally from a study of
transient changes in engine rotational speed following a disturbance in
fuel flow or propeller blade angle. The experimental results are com-
pared with the predicted values to check the reliability of the calcula-
tion method and the assumptions of a first-order linear system.

In the following discussion, attention is often directed to the
propeller and the engine as individual components or to the turboprop
engine as a unit. For the sake of clarity they will hereinafter be
differentiated and referred to as the propeller, the engine, and the
engine-propeller combination or, simply, combination.

Calculation of Time Constant for Engine-Propeller Combination

As stated in the ANALYSIS section, the torque-speed characteristics or the slopes of the torque-speed curve at constant blade angle and again at constant fuel flow were needed to complete the calculation of the combination time constant. In both cases, the steady-state torque-speed curves were based on the measured or shaft torque and hence included the gear-box losses.

The propeller characteristics were based on the torque of the propeller alone. Equations were derived to account for the gear-box losses, however, so that the values of shaft torque computed from equation (B10) of appendix B were consistent with the experimentally measured torque.

Propeller characteristics. - The generalized propeller characteristics are presented in figure 2, where the power coefficient C is plotted against the advance ratio $V/N_p D_p$. At each blade angle the power coefficient was defined as a distinct function of the advance ratio. Blade-angle lines without experimental data points were located by interpolation. The lines of constant blade angle were nearly parallel at high advance ratio and high blade angles, but at lower blade angles and advance ratio, the slope of the lines decreased. The effect upon the propeller torque-speed gain may be seen by considering each variable in the power coefficient $\dfrac{2\pi N_p Q_p}{\rho N_p^3 D_p^5}$ and the advance ratio $V/N_p D_p$, which are, respectively, $\dfrac{2\pi R^3 Q_p'}{D_p^5 \rho N_e^2}$ and $\dfrac{RV}{D_p N_e}$ when referred to the engine shaft.

At a given altitude and nominal engine speed, air density ρ and engine speed N_e are constant. Shifting to a lower velocity V along a constant-blade-angle line moves the power coefficient to a higher value where the slope of the curve decreases. Similarly, shifting to a lower velocity at a constant value of the power coefficient requires that the blade angle change from higher to lower values, which again results in curves with less slope. The propeller torque-speed gain $\left(\dfrac{\partial Q}{\partial N_e}\right)_\beta$, which varies with velocity V in a manner similar to the power coefficient, thus decreased with decreasing flight speed.

It was found that the power coefficient of this propeller at a given blade angle could be expressed empirically by a second-degree polynomial of the general form

$$C = \frac{2\pi R^3 Q_p'}{D_p^5 \rho N_e^2} = a + b\left(\frac{RV}{D_p N_e}\right) + c\left(\frac{RV}{D_p N_e}\right)^2$$

where a, b, and c are constants for a given blade angle as tabulated

in table II. From the equation for power coefficient, the equations for propeller torque and its first derivative with respect to engine rotational speed were derived. Including the gear-box losses as described in appendix B, the final equations (B10) and (B11) made possible the direct analytical evaluation of shaft torque and torque-speed gain $\left(\dfrac{\partial Q}{\partial N_e}\right)_\beta$ at any desired flight speed.

Torque-speed operating map. - The slope of the steady-state torque-speed curve for constant blade angles should be evaluated from data taken at constant flight conditions or at conditions identical to those from which the corresponding constant fuel-flow torque-speed data were obtained. The tunnel air speed varied, however, as the engine speed varied from one steady-state value to the next, and it varied in dissimilar ways during constant-blade-angle and constant-fuel-flow runs. The dissimilarity of tunnel air speed made it necessary to correct the experimental data taken during constant-blade-angle runs before a torque-speed operating map could be drawn.

The torque-speed characteristics fulfilling the requirements of identical simulated flight conditions during constant-fuel-flow and constant-blade-angle operation at an altitude of 35,000 feet and a Mach number of 0.45 are shown in figure 3. The lines of constant corrected fuel flow were obtained from steady-state data taken at the end points of blade-angle transients. The lines of constant blade angles were obtained from equation (B10) for shaft torque. Values of ρ and V used in the equation corresponded to those encountered at each engine speed during the constant-fuel-flow runs. The slopes of the constant-blade-angle lines $\left(\dfrac{\partial Q}{\partial N_e}\right)_\beta \dfrac{\sqrt{\theta}}{\delta}$ and the slopes of the constant-fuel-flow lines $\left(\dfrac{\partial Q}{\partial N_e}\right)_W \dfrac{\sqrt{\theta}}{\delta}$ provided the necessary information for calculating the combination time constant at this flight condition.

An examination of figure 3 indicates the probable trend to be expected in the values of the calculated time constants. The lines of constant blade angles are nearly straight and parallel. Hence the values of $\left(\dfrac{\partial Q}{\partial N_e}\right)_\beta \dfrac{\sqrt{\theta}}{\delta}$ are nearly equal for all blade angles.

The lines of constant fuel flow are lines of approximately constant power input or shaft horsepower. Because shaft horsepower is the product of torque and rotational speed, the value of shaft torque decreases as engine speed increases with fuel flow held constant. The slopes of the constant-fuel-flow lines are approximately equal for all values of corrected fuel flow and are also relatively small compared with the slopes

of the constant-blade-angle lines. The sum of the two slopes $\left(\dfrac{\partial Q}{\partial N_e}\right)_\beta \dfrac{\sqrt{\theta}}{\delta}$ and $\left(-\dfrac{\partial Q}{\partial N_e}\right)_W \dfrac{\sqrt{\theta}}{\delta}$, therefore, remains almost constant over the entire range of shaft horsepower. Consequently the calculated time constant may be expected to be almost invariant with shaft horsepower at the 35,000-foot, 0.45 Mach number condition.

Evaluation of the torque-speed gains required for time-constant calculation at flight Mach numbers other than 0.45 differed in procedure because insufficient constant-fuel-flow data precluded the plotting of torque-speed operating maps. The values of the gain $\left(\dfrac{\partial Q}{\partial N_e}\right)_W \dfrac{\sqrt{\theta}}{\delta}$ obtained from figure 3 were plotted against generalized engine speed as shown in figure 4. On the basis of extensive turbojet-engine experience (e.g., refs. 4 and 5), the assumption was made that gains describing the response of the engine operating at constant altitude generalize for different Mach numbers with the use of δ and θ. This assumption was borne out by the limited amount of constant-fuel-flow gain data obtained at various flight speeds and shown plotted in figure 4. A single curve is faired for the entire range of corrected fuel flows and flight Mach numbers covered. This curve provided the engine gain $\left(-\dfrac{\partial Q}{\partial N_e}\right)_W \dfrac{\sqrt{\theta}}{\delta}$.

The propeller gain $\left(\dfrac{\partial Q}{\partial N_e}\right)_\beta$ at various flight speeds was calculated by using equation (7) and substituting suitable values of V, ρ, and N_e for a given blade angle. The generalized values of the propeller gain thus calculated together with the engine gains $\left(-\dfrac{\partial Q}{\partial N_e}\right)_W \dfrac{\sqrt{\theta}}{\delta}$ from figure 4 provided the necessary information to calculate the time constant of the engine-propeller combination operating at flight Mach numbers of 0.15, 0.3, and 0.5 at an altitude of 35,000 feet.

Calculated time constant. - The calculated time constant of the engine-propeller combination in generalized form is plotted against generalized shaft horsepower in figure 5. The calculated points are included to show the degree of scatter given by the calculation technique. Flight Mach number had a marked effect on the value of the time constant. The effects of propeller blade angle and rotational speed combined, within limits, to make the engine time constant only a function of shaft horsepower at any given Mach number. The operational power level apparently had little effect upon the combination time constant at high Mach numbers, but the effect became more noticeable as flight speed decreased.

Another view of the variation in time constant with Mach number and power level is shown in figure 6, where the information of figure 5 is cross-plotted at values of constant shaft horsepower. The time constant increased 200 to 280 percent as the Mach number decreased from 0.5 to 0.15 with the larger increase occurring at the low power level.

Inasmuch as these values of time constant are calculated from equation (3), the variations in the time constant with power level and with flight Mach number can be traced to similar variations in one or both of the terms $\left(-\dfrac{\partial Q}{\partial N_e}\right)_W \dfrac{\sqrt{\theta}}{\delta}$ and $\left(\dfrac{\partial Q}{\partial N_e}\right)_\beta \dfrac{\sqrt{\theta}}{\delta}$. The variations in engine torque-speed gain $\left(-\dfrac{\partial Q}{\partial N_e}\right)_W \dfrac{\sqrt{\theta}}{\delta}$ are shown in figure 4 to be a function only of engine speed. Because the engine was operated over the entire normal range of rotational speed at any given flight Mach number, any variation in time constant caused by the variations in $\left(\dfrac{\partial Q}{\partial N_e}\right)_W \dfrac{\sqrt{\theta}}{\delta}$ would be expected to appear at a Mach number of 0.5 as well as at a Mach number of 0.15. Figure 6 shows, however, that the value of time constant was practically invariant at Mach 0.5. The dissimilar variation of time constant with power level at Mach numbers of 0.5 and 0.15 must therefore result from a corresponding variation in the propeller gains $\left(\dfrac{\partial Q}{\partial N_e}\right)_\beta \dfrac{\sqrt{\theta}}{\delta}$

It is significant to note that the combination time constant depends upon the sum of the engine gain and propeller gain, and therefore the relative numerical magnitude of the two gains is also an important factor.

The generalized torque-speed gain of the propeller calculated from equation (7) is shown in figure 7 plotted against generalized engine speed for various values of blade angle. The two blade-angle lines identified with the same symbol denote the approximate upper and lower values of blade angles covered during operation at that flight Mach number. The low blade angles were associated with the low flight speeds as were the high blade angles with high speeds. At any given flight speed the higher blade angle was associated with the high-shaft-horsepower operation. The variation in the gain due to a change in engine speed at any given blade angle did not exceed 9 percent over a corrected speed range of 2000 rpm. At a Mach number of 0.15 the variation in gain due to the change in power levels, that is, a change in blade angle, was about 47 percent at 15,000 rpm. At the same engine speed but at a Mach number of 0.3, the variation was reduced to 20 percent; at Mach 0.45, 8 percent; and at Mach 0.5, practically none. Thus the torque-speed gain of the propeller varied considerably with power level at the low Mach numbers and only slightly at the high flight speeds, which is consistent with the variation in the generalized time constant.

Because the time constant varies with the sum of the two gains $\left(-\dfrac{\partial Q}{\partial N_e}\right)_W \dfrac{\sqrt{\theta}}{\delta}$ and $\left(\dfrac{\partial Q}{\partial N_e}\right)_\beta \dfrac{\sqrt{\theta}}{\delta}$, their relative numerical values indicate the relative effects they have upon the combined response, as well as the predominance of one over the other at various operating conditions. At the higher Mach numbers, the propeller characteristics governed the variations in the value of the generalized combination time constant, because incremental changes in $\left(-\dfrac{\partial Q}{\partial N_e}\right)_W \dfrac{\sqrt{\theta}}{\delta}$, which is numerically small compared with $\left(\dfrac{\partial Q}{\partial N_e}\right)_\beta \dfrac{\sqrt{\theta}}{\delta}$, affect the sum of the two gains but slightly. As the air speed V increased, but the propeller rotational speed remained within a limited range, the propeller blade angle was obliged to vary in a manner such that the power requirement of the propeller matched the power available from the engine. The propeller characteristics were such that at the higher Mach numbers the propeller gain $\left(\dfrac{\partial Q}{\partial N_e}\right)_\beta$ had a tendency to approach a common value as shown in figure 7. The constant magnitude of the propeller gain irrespective of power level caused the time constant to likewise approach a common value as shown in figure 6.

At low flight speeds and correspondingly low blade angles, the engine gain and propeller gain were about equal in magnitude. Because shaft horsepower is a function of rotational speed and torque, the variation of engine gain with rotational speed and the variation of propeller gain with blade angle (or torque level) combined to cause the variation in time constant with power level at low Mach numbers.

The foregoing discussion also demonstrates the reason why the turboprop-engine time constant over a range of flight speeds does not generalize to a single curve when a parameter such as $\delta/\sqrt{\theta}$ is used. Flight speed and the attendant blade-angle change have dissimilar effects on the propeller gain $\left(\dfrac{\partial Q}{\partial N_e}\right)_\beta$ and the engine gain $\left(-\dfrac{\partial Q}{\partial N_e}\right)_W$. Thus the gains themselves as well as the sum of the two gains do not generalize to a single curve when a single parameter is used.

In contrast to the turboprop engine is the case of the turbojet engine. As pointed out in reference 5, the constants of the transfer functions, that is, gains and time constant at various altitudes and flight Mach numbers, generalized to one curve at standard static sea-level conditions.

An examination of equation (3) shows that generalization of the time constant of the engine-propeller combination to a single curve will require parameters which can be applied to the propeller gain and

the engine gain separately such that the sum of the two gains evaluated at different flight speeds will generalize to a single curve.

Determination of Time Constant from Transient Tests

Time constant evaluated from transient operation provide, by comparison with calculated results, validation of the calculation method of obtaining the combination time constant. In the calculation method, the engine is assumed to be a quasi-static system over the frequency range considered. Departures from this assumption, as well as the type and order of the response, can also be determined from studies of the results of the two methods.

Because of interaction of the turboprop engine and the wind tunnel, changes in engine operating speed caused dynamic variations in the simulated tunnel flight speed during a transient run. The effects of this interaction were taken into account in order that the calculated and experimental values of the time constant may be comparable. The method of correction for flight-speed variations and the effects upon response time are given in appendix B.

Blade-angle disturbances. - A typical recording of the transient response of the engine to a disturbance in the propeller blade angle is shown in figure 8. Engine fuel flow, propeller blade angle, torque, rotational speed, turbine-inlet total temperature, and tunnel dynamic pressure are the variables shown. This particular response was typical of the fastest disturbances attainable in blade angle and obviously did not approach too closely a step disturbance. Because step inputs were not attainable, semilog analysis could not be utilized. Instead, harmonic analysis with the aid of mechanical digital computers was performed to obtain the frequency-dependent engine characteristics (ref. 6). Typical results of amplitude ratio and phase shift of speed to blade angle are shown in figure 9. In figure 9(a) the amplitude ratio N_e/β is plotted against frequency. Values are nondimensionalized by dividing all values by the ratio obtained at the lowest frequency. The zero-frequency ratio of speed change to blade-angle change is the steady-state gain $\left(\frac{\partial N_e}{\partial \beta}\right)_W$. As frequency increases, the ratio tends toward zero. The value of ω when the amplitude ratio reaches 0.707 defines the break frequency ω_0. The engine time constant is determined by the relation $\tau = 1/\omega_0$. In figure 9(a) a theoretical first-order curve is drawn through the data points. In figure 9(b) the phase-shift characteristics are presented. Again a theoretical first-order curve is drawn with the 45° phase-shift point occurring at the same ω as the 0.707 point in figure 9(a). This information is combined in figure 9(c), where the theoretical first-order curve is drawn once more. The data from the harmonic analysis show that the response closely follows the theoretical first-order linear curves drawn in figure 9.

The time constants obtained from experimental transients are compared
with the calculated values and plotted against generalized shaft horse-
power in figure 10. The curves representing calculated results were
transferred from figure 5. At a Mach number of 0.45, sufficient experi-
mental results were available for comparison over the entire power range.
The values agreed well at the high-power end and deviated about 10 per-
cent at the low end. The combination time constant was invariant with
direction or size of disturbance to ±10 percent change in engine rotation-
al speed. At other Mach numbers, results for comparison were available
primarily in the high-power regions, but the agreement between calculated
and experimental results was good.

In summary, the similarity in trend as well as agreement between
the experimental and calculated results indicate that the assumptions
made previously are correct within the limits of accuracy of the data.
The engine held to quasi-static performance. The generalized engine gain
$\left(-\dfrac{\partial Q}{\partial N_e}\right)_W \dfrac{\sqrt{\theta}}{\delta}$ could be used for different flight Mach numbers at a given
altitude. The propeller characteristic curves and the empirical equations
describing them could be used to obtain the propeller gain $\left(\dfrac{\partial Q}{\partial N_e}\right)_\beta$ with
sufficient accuracy. These assumptions were applicable to input distur-
bances such as blade angle wherein departures from first-order linearity
were not encountered.

Fuel-flow disturbances. - The examination of engine transient per-
formance was completed by consideration of fuel-flow disturbances. A
typical transient is shown in figure 11. The fuel-flow trace shows that
the input closely approximated a true step and thus differed from the
blade-angle inputs. For the fuel-flow inputs, therefore, semilog rather
than harmonic analysis was utilized in the interest of economizing on
data reduction time.

During semilog analysis of the engine speed response, some charac-
teristics appeared which were not consistent with the experience obtained
on previously examined engines, thus indicating the occurrence of some
abnormal behavior in the engine. The analysis of the data was continued
by the semilog method and several representative results were checked and
verified by the harmonic analysis method.

The generalized time constant of the engine-propeller combination
obtained from the fuel-flow-step data are shown in figure 12 plotted
against generalized shaft horsepower. The same trends with horsepower
and Mach number were evident here as in the time constant shown in figures
5 and 10. The degree of scatter was comparable and, as in the case of
blade-angle disturbances, no effect of step size or direction was evident.
The values of time constant obtained from fuel-flow steps were, however,
30 to 50 percent larger than those obtained from blade-angle disturbances
and from the calculation method.

Gas-turbine engines considered previously have, in response to fuel-step disturbances, exhibited a sharp initial temperature rise followed by an exponential decay to a final value. Examination of the turbine-inlet temperature response, of which figure 11 is typical, shows that in the present engine the response is decidedly different. In addition, the rotational speed response shows an unexpected long-term drift in the direction of the fuel disturbance. Such behavior indicates a departure from quasi-static performance during response to a fuel-flow step. This departure is believed to be caused by transients in the combustion process or possibly transient changes in the engine internal-flow conditions and geometry.

The experimental data and information necessary to describe the physical phenomena and to determine the causes of a departure from quasi-static performance are not available from the present investigation. With the assumption, however, that the internal engine dynamics are the cause of the 30- to 50-percent difference in time constant between fuel-flow and blade-angle disturbances, the variation in time constant due to flight speed should be similar in trend and in magnitude regardless of the type of disturbance. This similarity should be especially true in regions of operation where the propeller characteristics are the controlling factor in the value of the combination time constant. A brief examination of the magnitude of variations in time constant at a given shaft horsepower for both the blade-angle and fuel-flow disturbances shows this to be the case.

SUMMARY OF RESULTS

The following results were obtained from the altitude-wind-tunnel investigation of a turboprop engine conducted at a simulated altitude of 35,000 feet over a flight Mach number range of 0.15 to 0.5.

The propeller performance characteristics, expressed as power coefficient and advance ratio, were useful in prediction of the system time constant at various flight speeds.

Generalized time constant of the engine-propeller combination varied with power level and flight speed. At any given flight condition within the range investigated, the time constant was found to be a function only of power level. The variation with flight speed was in the order of 200- to 280-percent increase in the generalized time constant, depending on the operating power level, as flight Mach number decreased from 0.5 to 0.15.

For both blade-angle and fuel-flow inputs, the system time constant was invariant with direction or size of disturbance to ±10 percent speed change. The calculated time constant agreed with the experimental time

constant obtained from blade-angle transients. The time constant obtained from the fuel-flow transients, however, was 30 to 50 percent larger than that obtained from blade-angle transients. This is believed to be caused by transients in the combustion process or possibly transient changes in the engine internal flow conditions and geometry.

The trend and magnitude of the flight-speed effects on time constant were similar for both the fuel-flow and blade-angle disturbances.

Lewis Flight Propulsion Laboratory
    National Advisory Committee for Aeronautics
        Cleveland, Ohio, January 18, 1955

APPENDIX A

SYMBOLS

The following symbols are used in this report:

a   constant

b   constant

C   power coefficient

c   constant

D   diameter, ft

HP   horsepower

h   constant

I   polar moment of inertia

l constant

M   Mach number

m   constant

N   rotational speed, rev/sec or rev/min

n   constant

Q   torque, lb-ft

R   reduction gear-box speed ratio

S   Laplace operator

SHP   shaft horsepower

V   free-stream air velocity, ft/sec

W   fuel flow, lb/hr

β propeller blade angle, deg

δ ratio of absolute total pressure at engine inlet to NACA standard
         atmospheric pressure at sea-level static conditions

θ ratio of absolute total temperature at engine inlet to NACA stand-
         ard atmospheric temperature at sea-level static conditions

ρ air density, slugs/cu ft

τ time constant, sec

ω frequency, radians/sec

ω_0 break frequency, radians/sec

Subscripts:

e   engine

i   indicated

L   gear-box losses

p   propeller

Superscript:

'   referred to engine shaft

APPENDIX B

DERIVATION OF EQUATIONS FOR ANALYSIS OF DATA

Propeller Equations

The equation for propeller power coefficient as an empirical function of advance ratio is

$$C = \frac{2\pi N_p Q_p}{\rho N_p^3 D_p^5} = a + b\left(\frac{V}{N_p D_p}\right) + c\left(\frac{V}{N_p D_p}\right)^2$$

where a, b, and c are constants for a given blade angle and are given in table II. By referring propeller torque and rotational speed to the engine shaft by means of the relations

$$\frac{N_e}{N_p} = R = 12.5$$

and

$$N_p Q_p = N_p' Q_p' = N_e Q_p'$$

the equation for the power coefficient becomes

$$C = \frac{2\pi R^3 N_e Q_p'}{D_p^5 \rho N_e^3} = a + b\left(\frac{RV}{D_p N_e}\right) + c\left(\frac{RV}{D_p N_e}\right)^2 \tag{B1}$$

The characteristic of the propeller ultimately desired for the purpose of calculating the time constant is the propeller torque-speed gain $\left(\frac{\partial Q}{\partial N_e}\right)_\beta$. An expression for torque as a function of rotational speed is first obtained by solving equation (B1) for Q_p' and combining the constants; thus,

$$Q_p' = l\rho N_e^2 + m\rho V N_e + n\rho V^2 \tag{B2}$$

Taking partial derivatives with respect to N_e gives

$$\left(\frac{\partial Q_p'}{\partial N_e}\right)_{\beta,\rho,V} = \rho(2lN_e + mV) \tag{B3}$$

The total horsepower at the shaft is the sum of the propeller horsepower and the horsepower due to the gear-box losses:

$$SHP = (HP)_p' + (HP)_L \tag{B4}$$

But from manufacturer's data, $(HP)_L$ at a 35,000-foot altitude can be empirically expressed as

$$(HP)_L = h(HP)_p' + 0.212N_e - 29.4 \tag{B5}$$

where $h = 0.005$. The general equation for torque from horsepower is

$$Q = \frac{550HP}{2\pi N} \tag{B6}$$

Multiplying equation (B4) by 550 and dividing by $2\pi N_e$ yield

$$\frac{550SHP}{2\pi N_e} = \frac{550(HP)_p'}{2\pi N_e} + \frac{550(HP)_L}{2\pi N_e} \tag{B7}$$

or, in terms of torque,

$$Q = Q_p' + Q_L \tag{B8}$$

But from equations (B6) and (B5), Q_L can be obtained as

$$\left.\begin{aligned}
Q_L &= \frac{550(HP)_L}{2\pi N_e} \\[1em]
&= \frac{550}{2\pi N_e}\left[h(HP)_p' + 0.212N_e - 29.4\right] \\[1em]
&= \frac{550h(HP)_p'}{2\pi N_e} + \frac{550\times 0.212N_e}{2\pi N_e} - \frac{29.4\times 550}{2\pi N_e} \\[1em]
&= hQ_p' + 18.557 - \frac{2573.5}{N_e}
\end{aligned}\right\} \tag{B9}$$

Substituting equation (B9) into (B8) gives

$$\left.\begin{aligned}
Q &= Q_p' + hQ_p' - \frac{2573.5}{N_e} + 18.557 \\[1em]
&= (1 + h)Q_p' - \frac{2573.5}{N_e} + 18.557
\end{aligned}\right\} \tag{B10}$$

Taking the partial derivative of equation (B10) with respect to N_e yields

$$\left(\frac{\partial Q}{\partial N_e}\right)_\beta = (1 + h)\left(\frac{\partial Q_p'}{\partial N_e}\right)_\beta + \frac{2573.5}{N_e^2} \qquad (B11)$$

where $\left(\partial Q_p'/\partial N_e\right)_\beta$ is given by equation (B3).

Equation (B11) is the mathematical representation for the torque-speed gain of the propeller at a given blade angle. The gain is evaluated by substituting the values of ρ, V, and N_e prevalent during a given simulated flight condition. It is then generalized by the corresponding values of $\sqrt{\theta/\delta}$. The resulting generalized gain is equivalent to the slope of the steady-state curve of generalized shaft torque plotted against generalized engine speed.

Correction for Transient Variation in Wind-Tunnel Air Velocity

The wind tunnel and the propeller of the turboprop engine may be considered a closed energy system in equilibrium during a steady-state run. A sudden change in propeller rotational speed during a transient run, whether brought about by a fuel-flow or blade-angle disturbance, causes a permanent or temporary shift (depending on type of disturbance) in the equilibrium of the system. The shift in equilibrium is manifested in a change in the tunnel air velocity approaching the propeller. This interaction of the tunnel and propeller varies with the type of disturbance and flight condition and has a decided influence on the response time of the engine. Performance at a constant Mach number was used as a common reference, and all experimental transients were corrected to this base.

The correction for fuel-flow disturbances is similar to that made in reference 5. Tunnel dynamic pressure and, hence, tunnel air speed vary with engine speed. An additional term may thus be added to equation (3) giving the following equation for the time constant including the effects of a change in air speed:

$$\tau_i = \frac{I_e + I_p'}{\left(\frac{\partial Q}{\partial N_e}\right)_\beta + \left(-\frac{\partial Q}{\partial N_e}\right)_W + \left(-\frac{\partial Q}{\partial V}\frac{\partial V}{\partial N_e}\right)} \qquad (B12)$$

The time constant τ_i may be considered as representing the experimentally indicated time constant with a varying air speed in contrast with

τ from equation (3) representing the time constant with constant air speed. Taking the ratio of time constants gives

$$\frac{\tau}{\tau_i} = \frac{\left(\frac{\partial Q}{\partial N_e}\right)_\beta + \left(\frac{\partial Q}{\partial N_e}\right)_W + \left(-\frac{\partial Q}{\partial V}\frac{\partial V}{\partial N_e}\right)}{\left(\frac{\partial Q}{\partial N_e}\right)_\beta + \left(-\frac{\partial Q}{\partial N_e}\right)_W} \tag{B13}$$

If the quantity K represents the sum of the two gain terms $\left(\frac{\partial Q}{\partial N_e}\right)_\beta + \left(-\frac{\partial Q}{\partial N_e}\right)_W$ characteristic of any given steady-state operating point, then

$$\frac{\tau}{\tau_i} = \frac{K + \left(-\frac{\partial Q}{\partial V}\frac{\partial V}{\partial N_e}\right)}{K} = 1 + \frac{1}{K}\left(-\frac{\partial Q}{\partial V}\frac{\partial V}{\partial N_e}\right) \tag{B14}$$

The experimentally obtained time consant corrected for varying air speed becomes

$$\tau = \tau_i\left[1 + \frac{1}{K}\left(-\frac{\partial Q}{\partial V}\frac{\partial V}{\partial N_e}\right)\right] \tag{B15}$$

The term $\left(-\frac{\partial Q}{\partial V}\frac{\partial V}{\partial N_e}\right)$ was evaluated by obtaining $\left(\frac{\Delta V}{\Delta N_e}\right)_{W,\beta}$, the change in flight speed with rotational speed, and multiplying it by $\left(-\frac{\Delta Q}{\Delta V}\right)_\beta$, the change in torque due to the change in flight speed. This correction became significant as the Mach number is increased, and in some cases amounted to a decrease of 20 to 30 percent in response time.

In the case of propeller blade-angle changes, the tunnel flight speed also varies but not directly with engine rotational speed. After a perturbation in blade angle, the characteristic time of the tunnel's adjustment to the new blockage conditions is considerably longer than the engine response time. Thus, the corrections for test-facility effects on results obtained from blade-angle disturbances were different from those used for fuel-flow steps.

Upon examination of a number of transient responses, the tunnel dynamic pressure was found to have consistent characteristics; thus, it is possible to approximate the tunnel response mathematically. With this expression and the use of the propeller curves of figure 2, equivalent blade angles along a simulated constant-tunnel-velocity transient were

determined. The equivalent blade angles along the simulated transient pro-
duced engine loading, or torque, equal to that obtained at the experimental
conditions, which were not at constant tunnel velocity. A subsequent
analysis of engine response to the equivalent blade-angle disturbances by
use of an analog computer showed that the experimental time responses at an
altitude of 35,000 feet and a Mach number of 0.45 were consistently 20-
percent slower than those that would be obtained for the same engine in
a noninteracting test facility. This correction factor, therefore, was
evaluated at each Mach number and applied to all the experimental results
obtained from blade-angle transients.

REFERENCES

1. Krebs, Richard P., Himmel, Seymour C., Blivas, Darnold, and Shames,
     Harold: Dynamic Investigation of Turbine-Propeller Engine under
     Altitude Conditions. NACA RM E50J24, 1950.

2. Taylor, Burt L., III, and Oppenheimer, Frank L.: Investigation of
     Frequency-Response Characteristics of Engine Speed for a Typical
     Turbine-Propeller Engine. NACA Rep. 1017, 1951. (Supersedes NACA
     TN 2184.)

3. Oppenheimer, Frank L., and Jacques, James R.: Investigation of Dy-
     namic Characteristics of a Turbine-Propeller Engine. NACA RM
     E51F15, 1951.

4. Craig, R. T., Vasu, George, and Schmidt, R. D.: Dynamic Character-
     istics of a Single-Spool Turbojet Engine. NACA RM E53C17, 1953.

5. Delio, Gene J., and Rosenzweig, Solomon: Dynamic Response at Altitude
     of a Turbojet Engine with Variable Area Exhaust Nozzle. NACA RM
     E51K19, 1952.

6. Delio, Gene J.: Evaluation of Three Methods for Determining Character-
     istics of a Turbojet Engine. NACA TN 2634, 1952.

TABLE I. - INSTRUMENTATION

Measured quantity	Steady-state instrumentation	Transient instrumentation	
		Sensor	Frequency range, cps
Fuel flow	Rotameter	Aneroid-type pressure sensor, with strain-gage element, connected to measure pressure drop across variable orifice in fuel line	0 to 60
Blade angle	Slide-wire on propeller and connected in electric circuit to give indication on microammeter	Slide-wire on propeller	0 to 100
Engine speed	Modified electronic digital counter with frequency-generating tachometer	Shaped frequency signal from counter integrated with respect to time.	0 to 35
Thrust	Calibrated bridge balance on strain analyzer	Strain gage and like attached to engine mounting frame	0 to 100
Torque	Electronic measurement with reluctance pickups of twist in drive shaft between compressor and gear box. Indication of twist given on calibrated self-balancing potentiometer.	Steady-state instrumentation modified to give transient indication	0 to 80
Turbine-inlet temperature	Nine individual thermocouples connected to self-balancing recorder	Four paralleled 20-gage chromel-alumel thermocouples and electric network to compensate for thermocouple lag	0 to 25 at sea level when used with properly adjusted compensator
Turbine-outlet temperature	Sixteen individual thermo-couples connected to self-balancing recorder.	Eight paralleled 20-gage chromel-alumel thermocouples and electric network to compensate for thermocuple lag	0 to 15 at sea level when used with properly adjusted compensator
Tunnel dynamic pressure	Water manometers	Aneroid-type pressure sensor, with strain-gage element	Damping ratio of 0.5, and damped natural frequency of 20 cps at 15,000 ft
Engine air flow	Water manometers	Diaphragm-type pressure sensor, with strain-gage element	Damping ratio of 0.5, and damped natural frequency of 20 cps at 15,000 ft
Compressor-inlet total pressure	Water manometers	Diaphragm-type pressure sensor, with strain-gage element	
Compressor-outlet total pressure	Mercury manometers	Aneroid-type pressure sensor, with strain-gage element	

TABLE II. - COEFFICIENTS FOR PROPELLER

CHARACTERISTIC EQUATION

$$C = \frac{2\pi N_p Q_p}{\rho N_p^3 D_p^5} = a + b \left(\frac{V}{N_p D_p}\right) + c \left(\frac{V}{N_p D_p}\right)^2$$

Propeller blade angle, β, deg	a	b	c
28	0.1427	0.1997	-0.3375
30	.1384	.2643	-.3470
31.5	.1598	.2374	-.3061
32	.0995	.3766	-.3737
34	.1796	.2417	-.2833
36.5	.2345	.2195	-.2582
38	.2310	.2678	-.2683
40	.2291	.3243	-.2771
40.7	.2842	.2578	-.2473
42	.5106	.0680	-.1975
44	.4615	.1814	-.2207
45	.5151	.1830	-.2238
46	.2165	.5648	-.3288
47	.4448	.4053	-.2933
47.75	.1397	.7617	-.3833
49	-.3294	1.2384	-.4833
50.5	-.0270	.9165	-.3750

C-33310
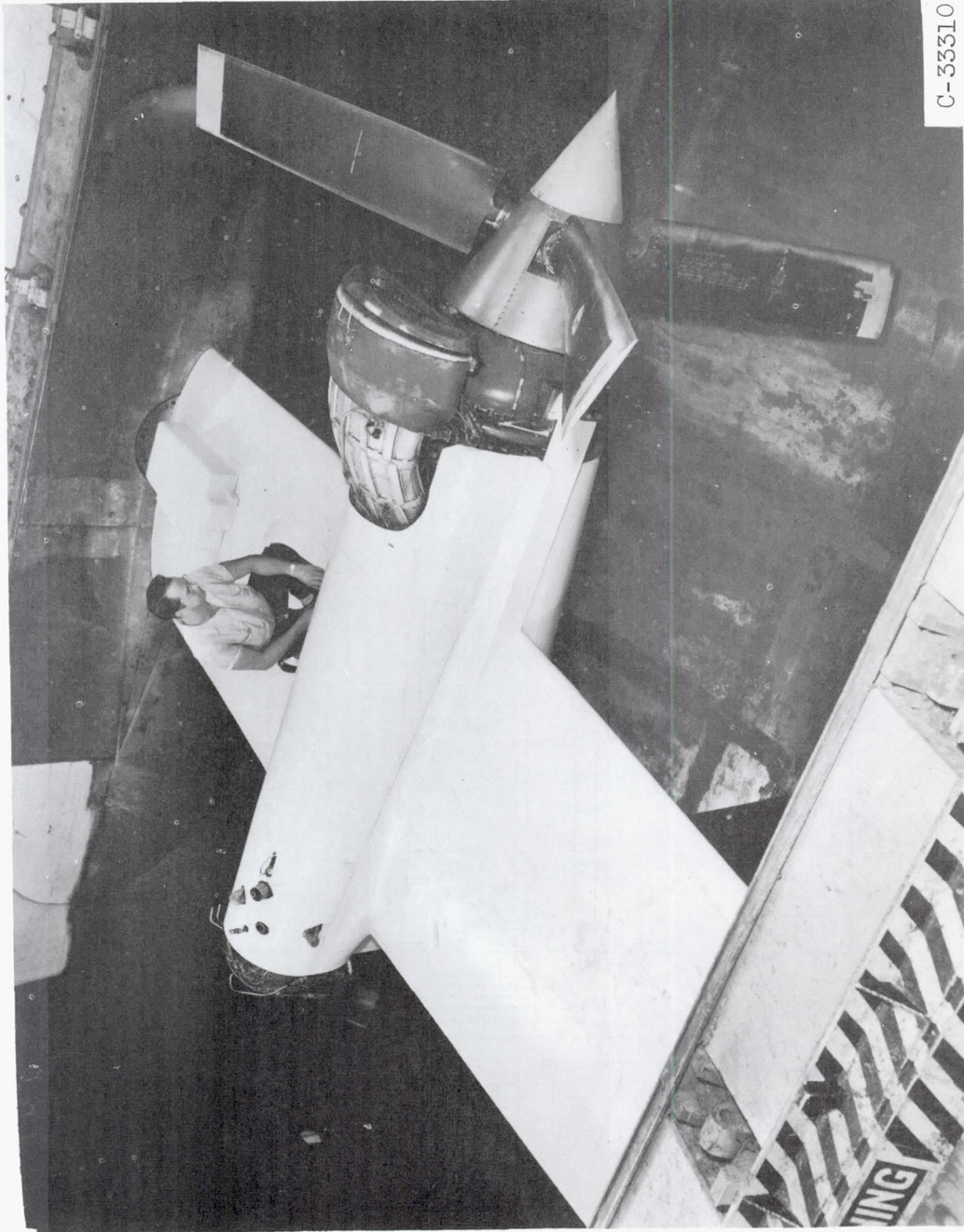
(a) Wind-tunnel installation.

Figure 1. - Turboprop engine.
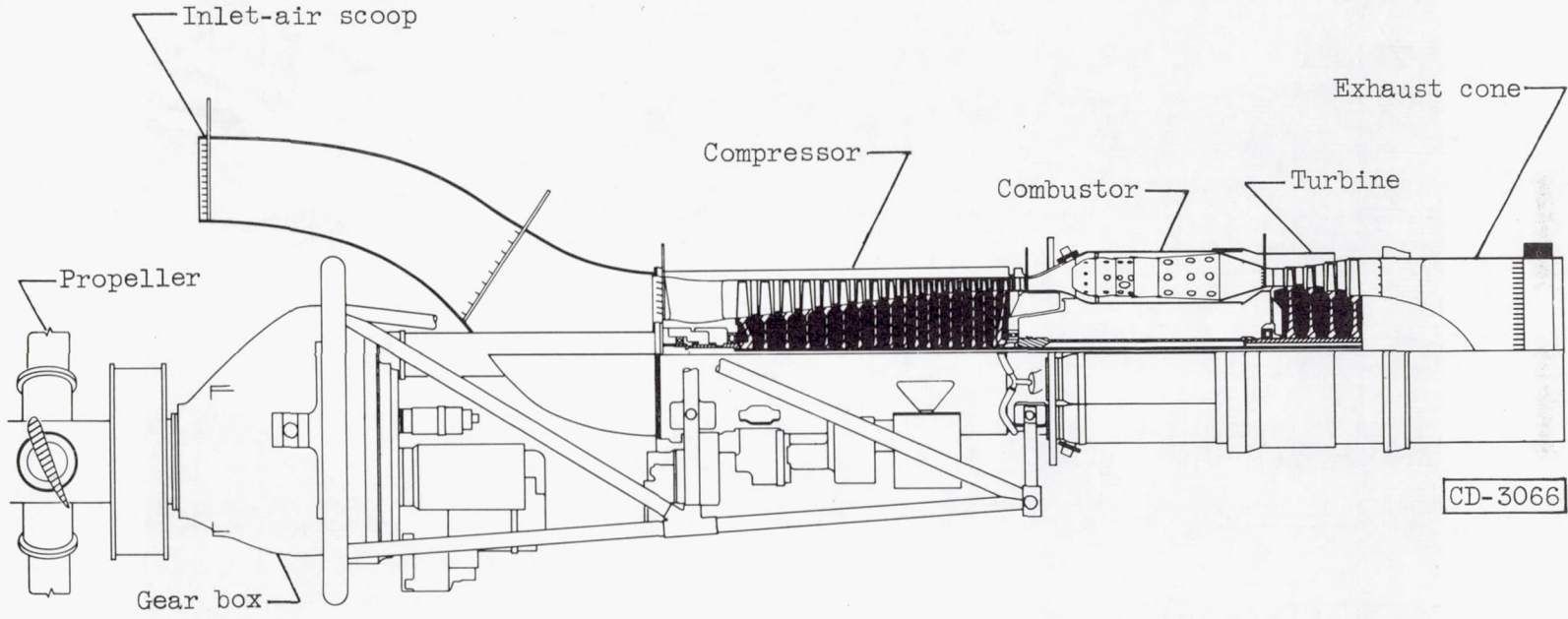
(b) Schematic cross section and components.

Figure 1. - Concluded. Turboprop engine.
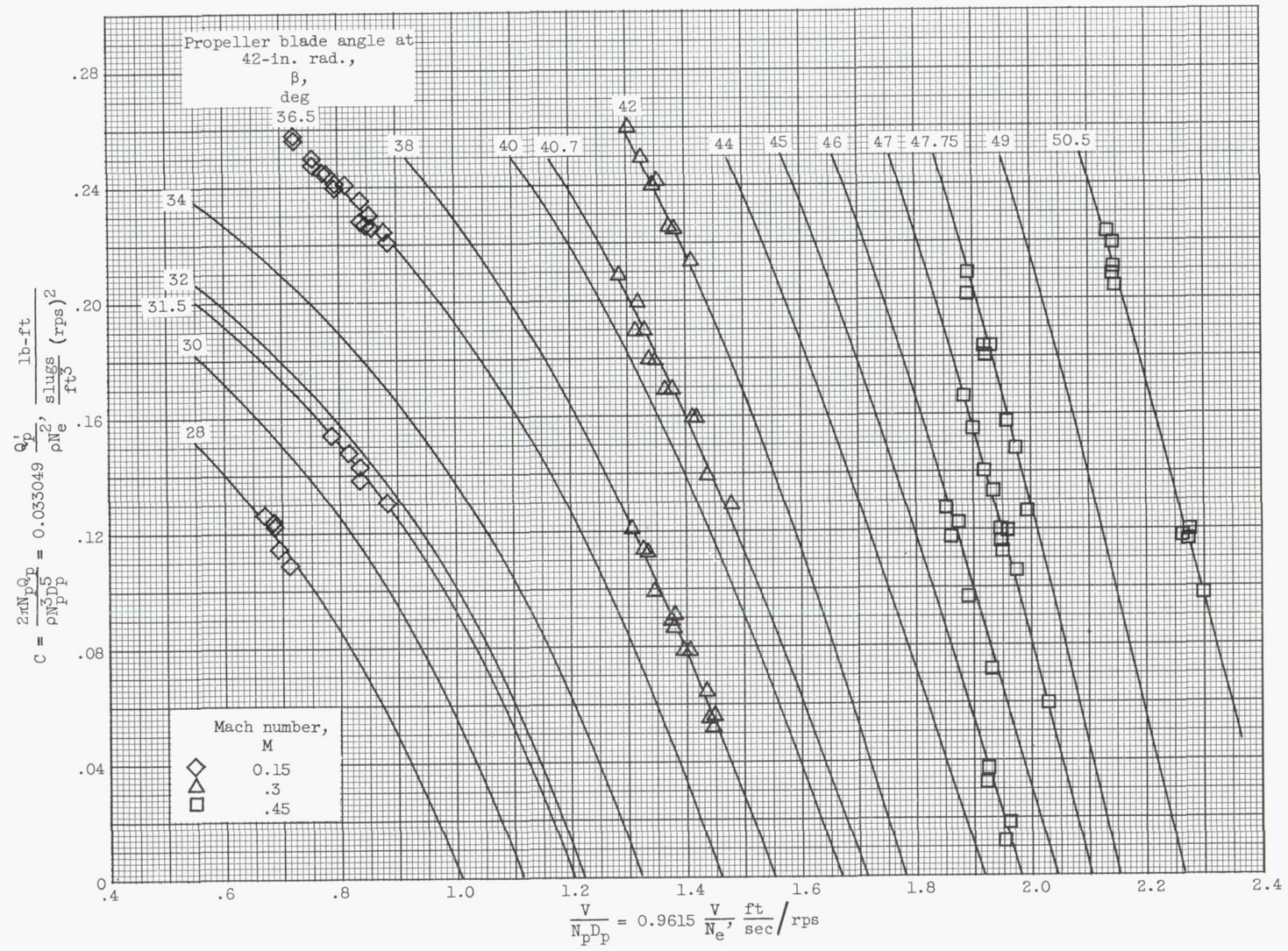
Figure 2. - Propeller power coefficient - advance ratio characteristics.
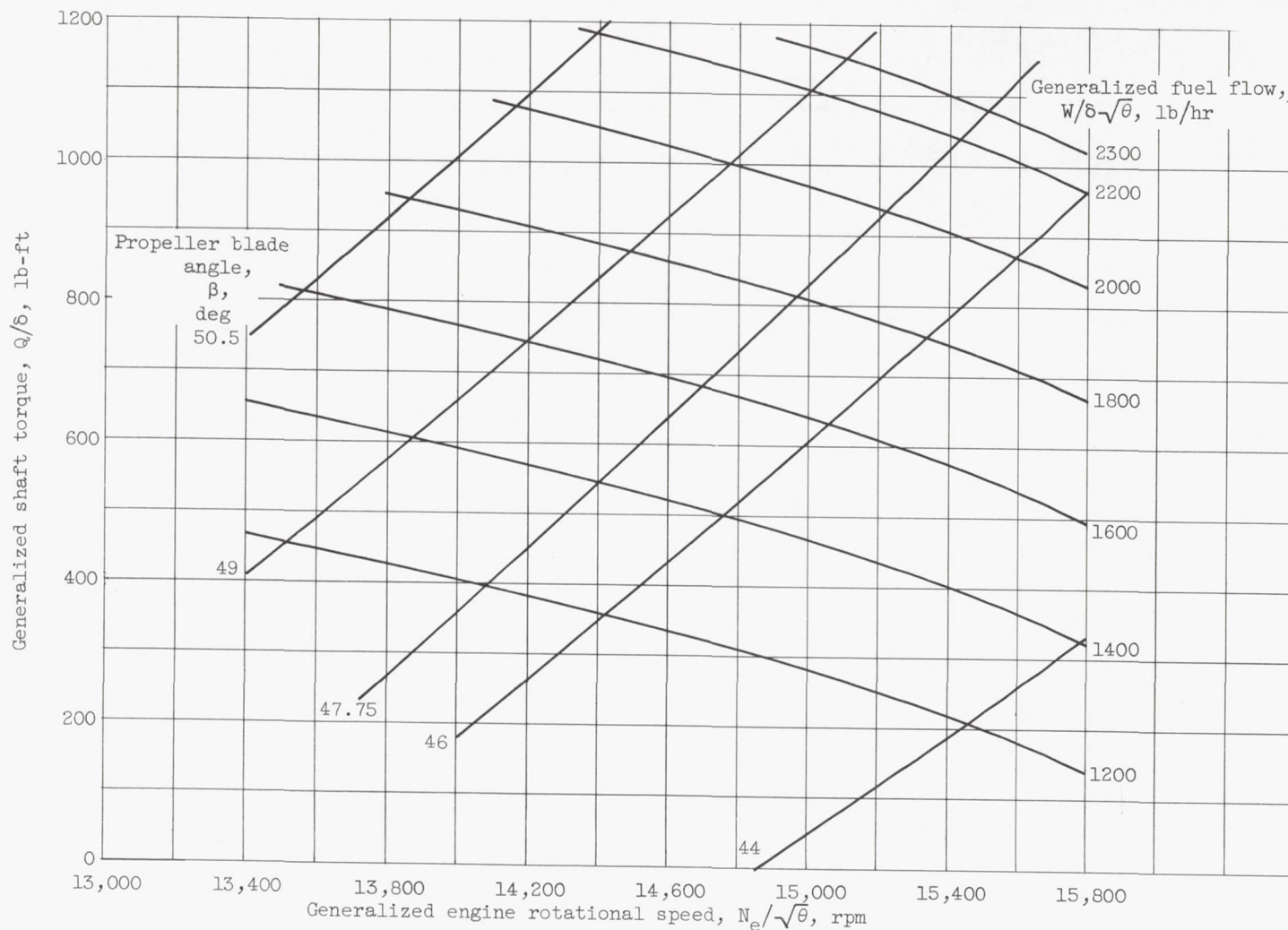
Figure 3. - Variation of generalized shaft torque with generalized engine speed. Altitude, 35,000 feet; Mach number, 0.45.
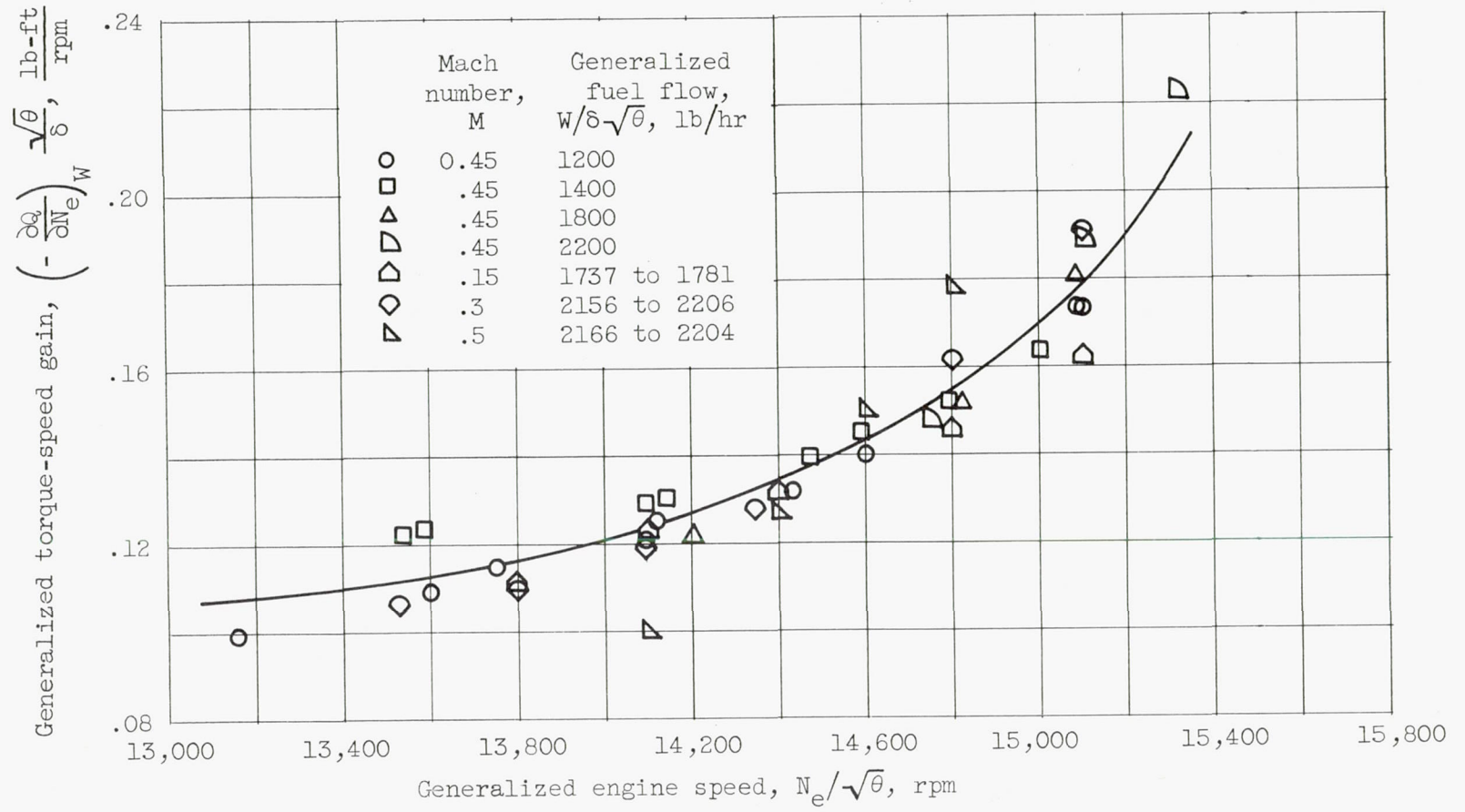
Figure 4. - Variation of generalized torque-speed gain with generalized speed at various Mach numbers. Altitude, 35,000 feet.
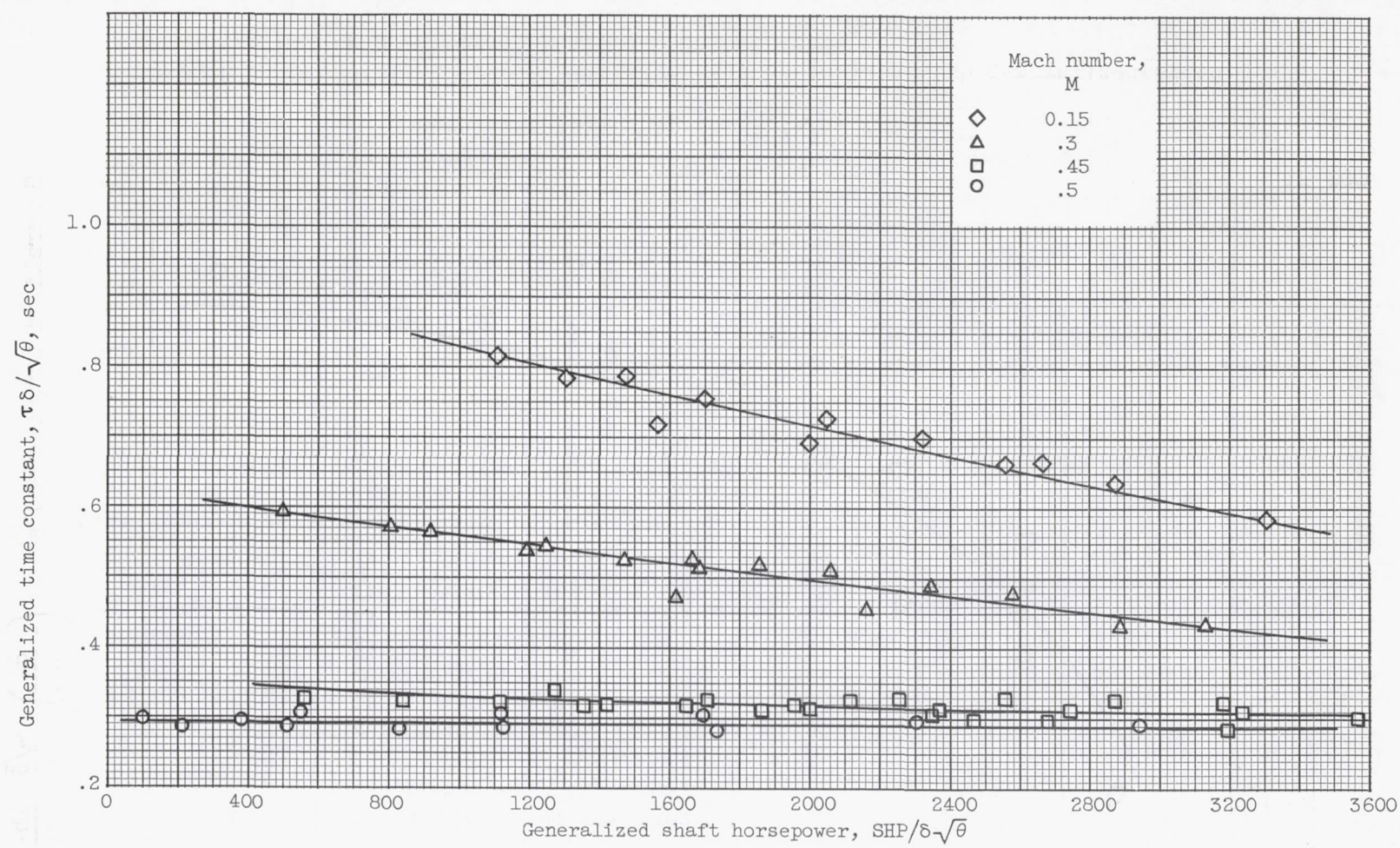
Figure 5. - Variation of generalized time constant with shaft horsepower. Altitude, 35,000 feet. (Time constant calculated from steady-state characteristics.)
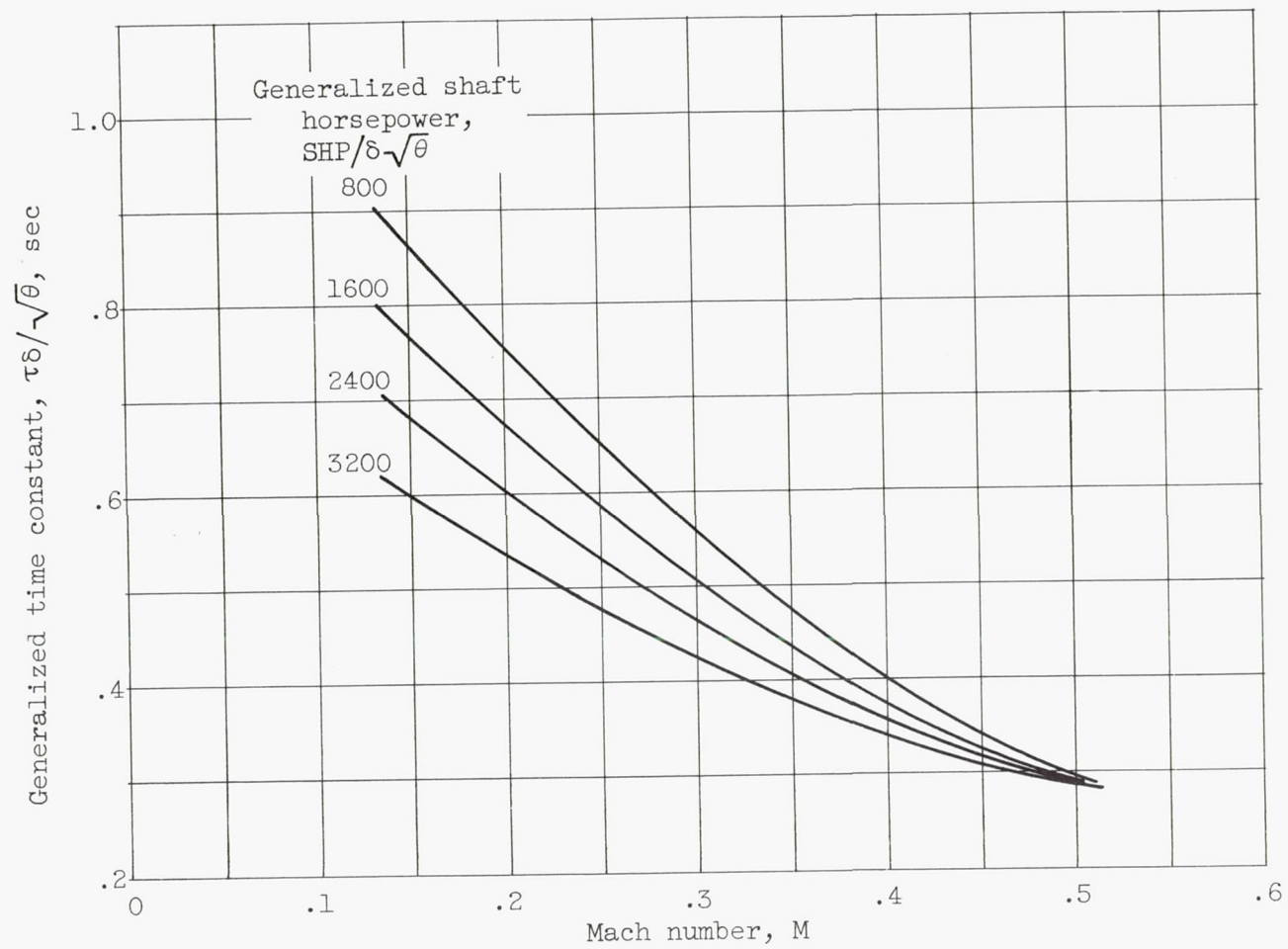
Figure 6. - Variation of generalized time constant with Mach number.
Altitude, 35,000 feet. (Time constant calculated from steady-state
characteristics.)
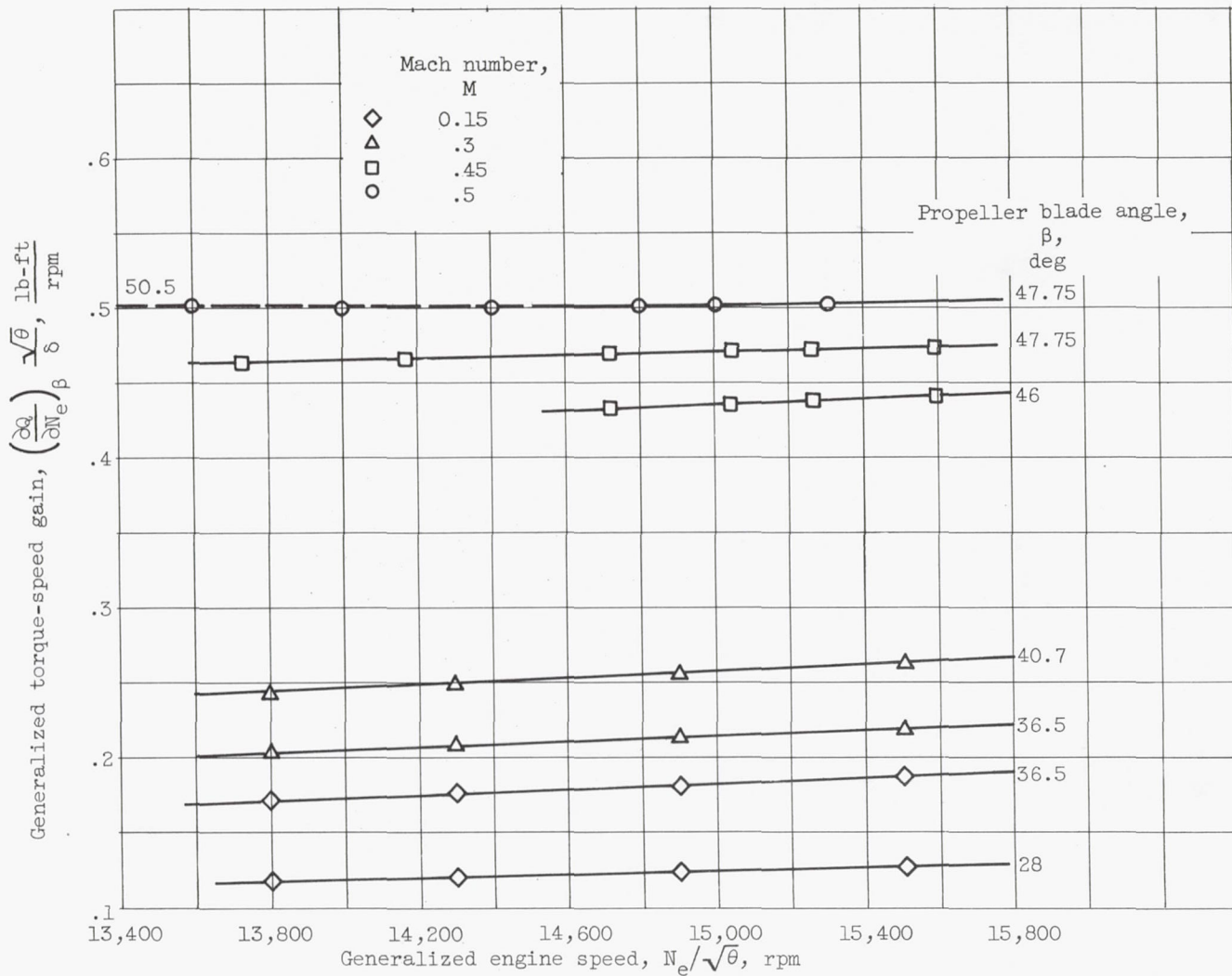
Figure 7. - Variation of generalized torque-speed gain with engine speed at various Mach numbers and propeller blade angles.

(a) Fuel flow.

(b) Blade angle.

(c) Torque.

(d) Engine speed.

(e) Turbine-inlet temperature.

(f) Tunnel dynamic pressure.
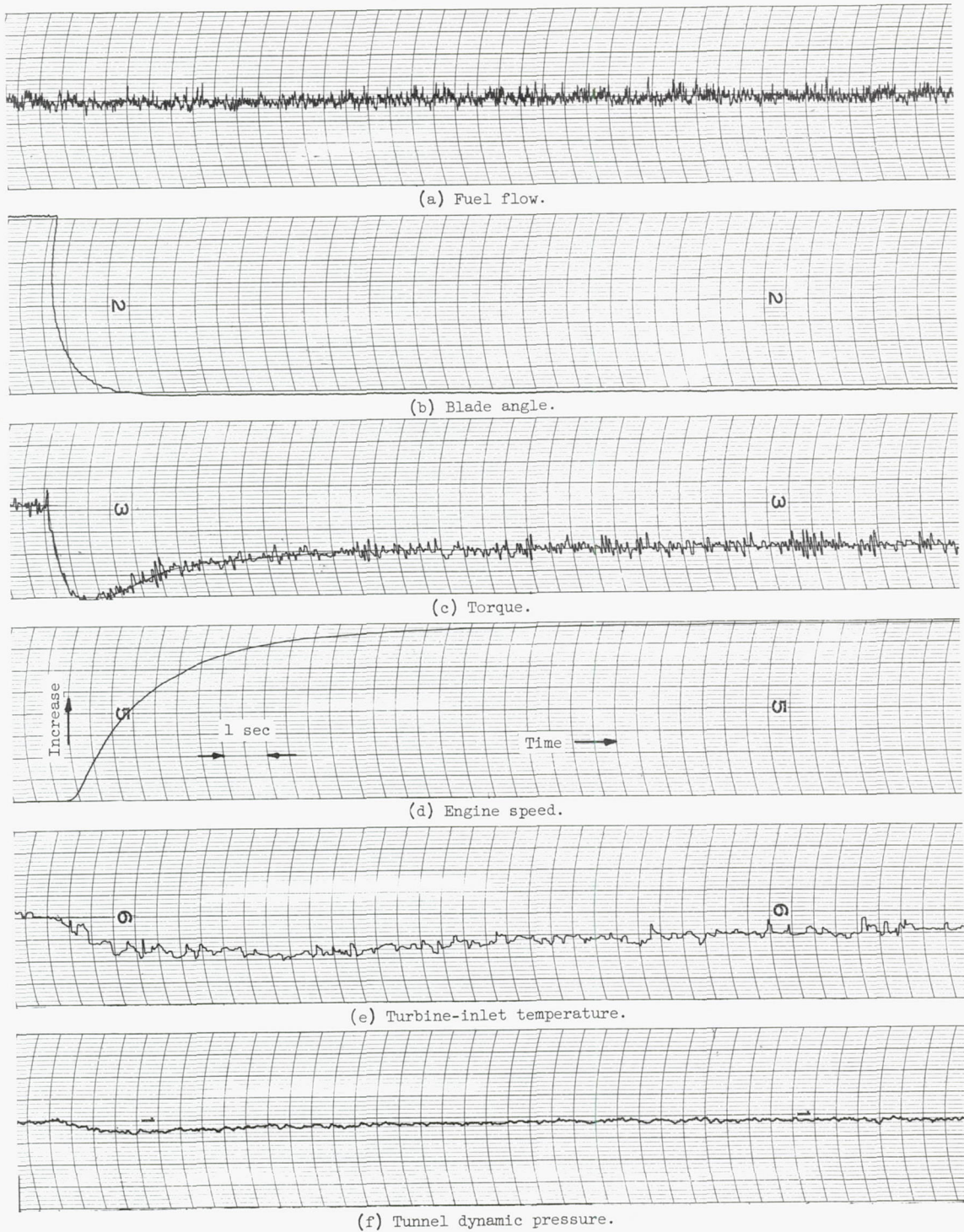
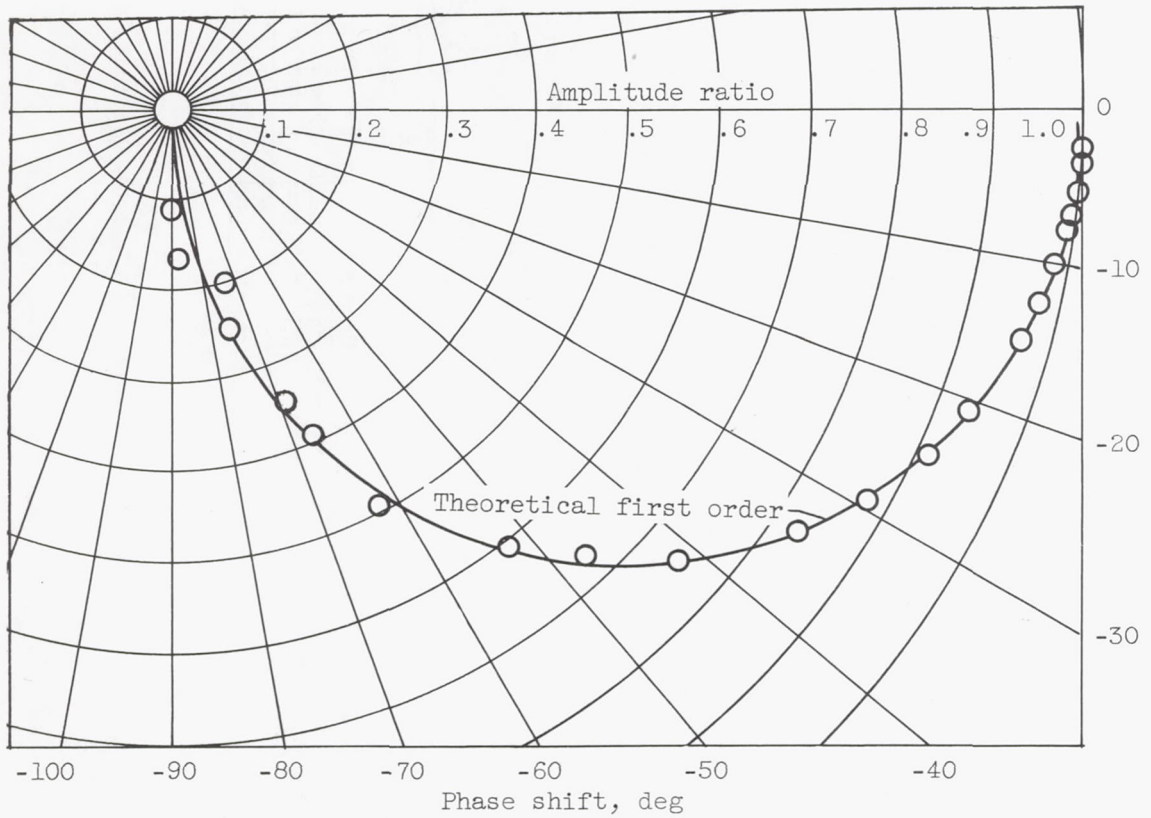Figure 8. - Transient response of engine to blade-angle disturbance. Altitude, 35,000 feet; Mach number, 0.45.
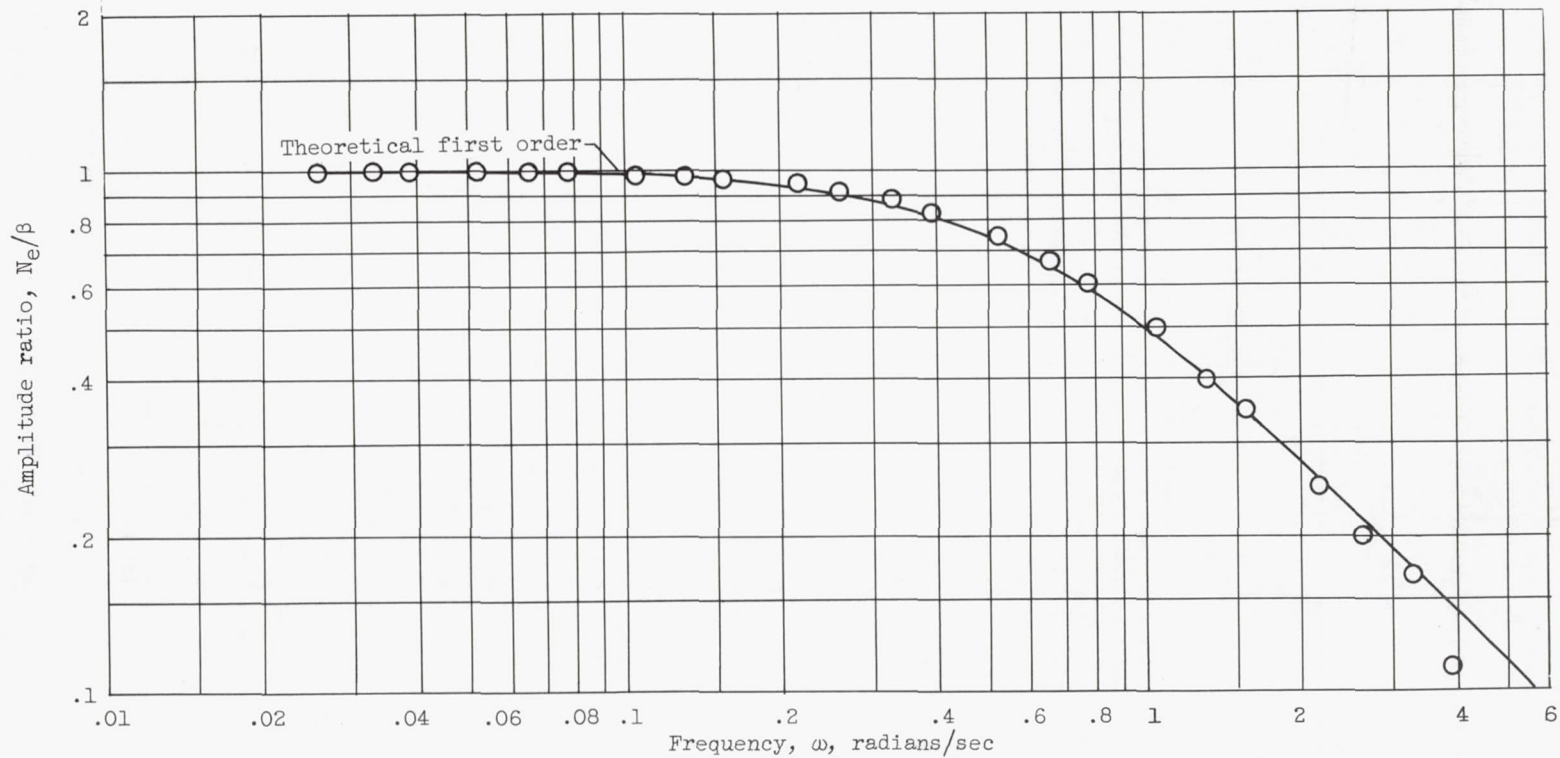
(a) Amplitude ratio.

Figure 9. - Frequency response of engine speed to propeller blade angle.   Altitude, 35,000 feet; Mach number, 0.45;
12-percent change in rotational speed.
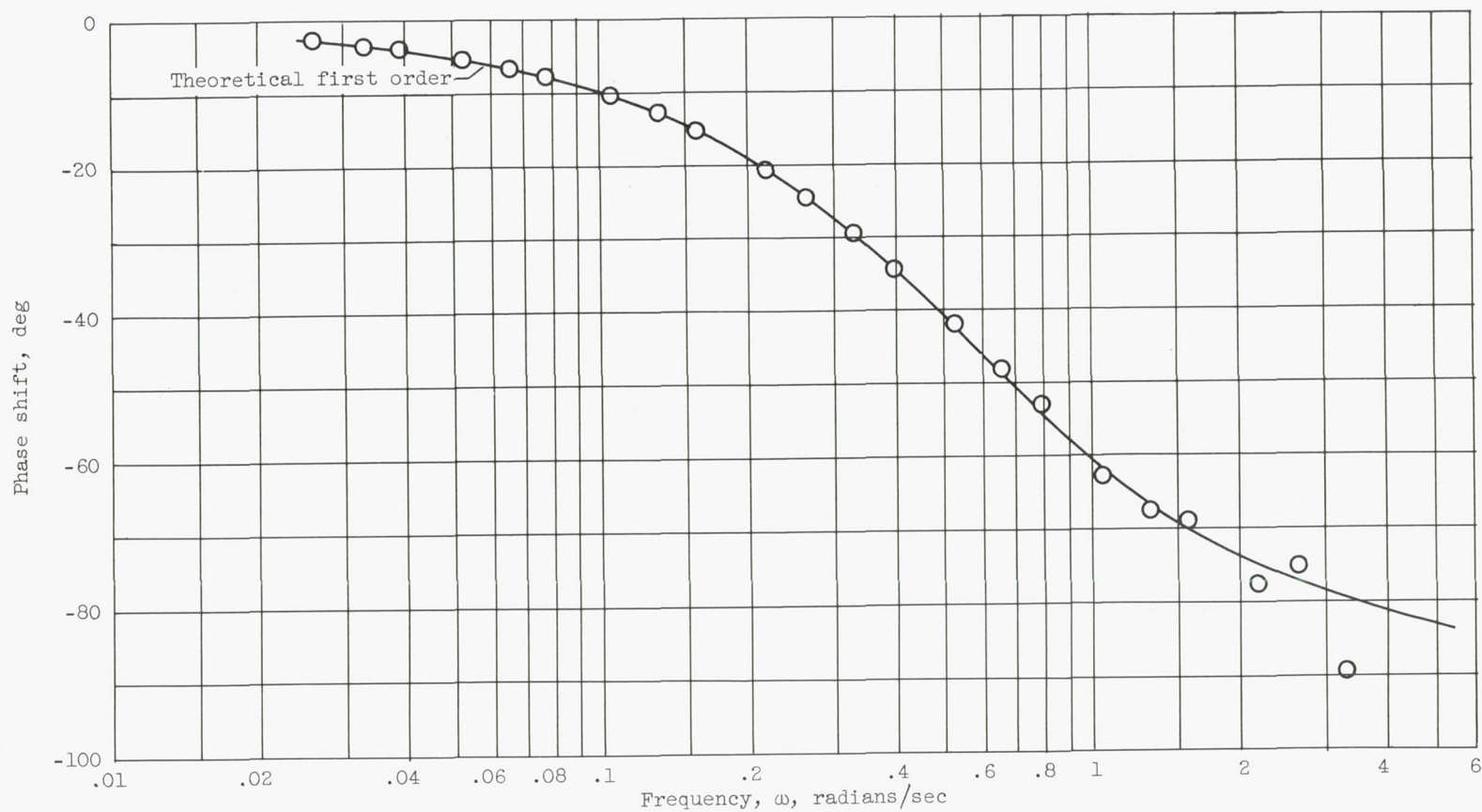
(b) Phase shift.

Figure 9. - Continued.   Frequency response of engine speed to propeller blade angle.   Altitude, 35,000 feet; Mach number, 0.45; 12-percent change in rotational speed.

(c) Phase shift - amplitude ratio relation.

Figure 9. - Concluded. Frequency response of engine speed to propeller
    blade angle. Altitude, 35,000 feet; Mach number, 0.45; 12-percent
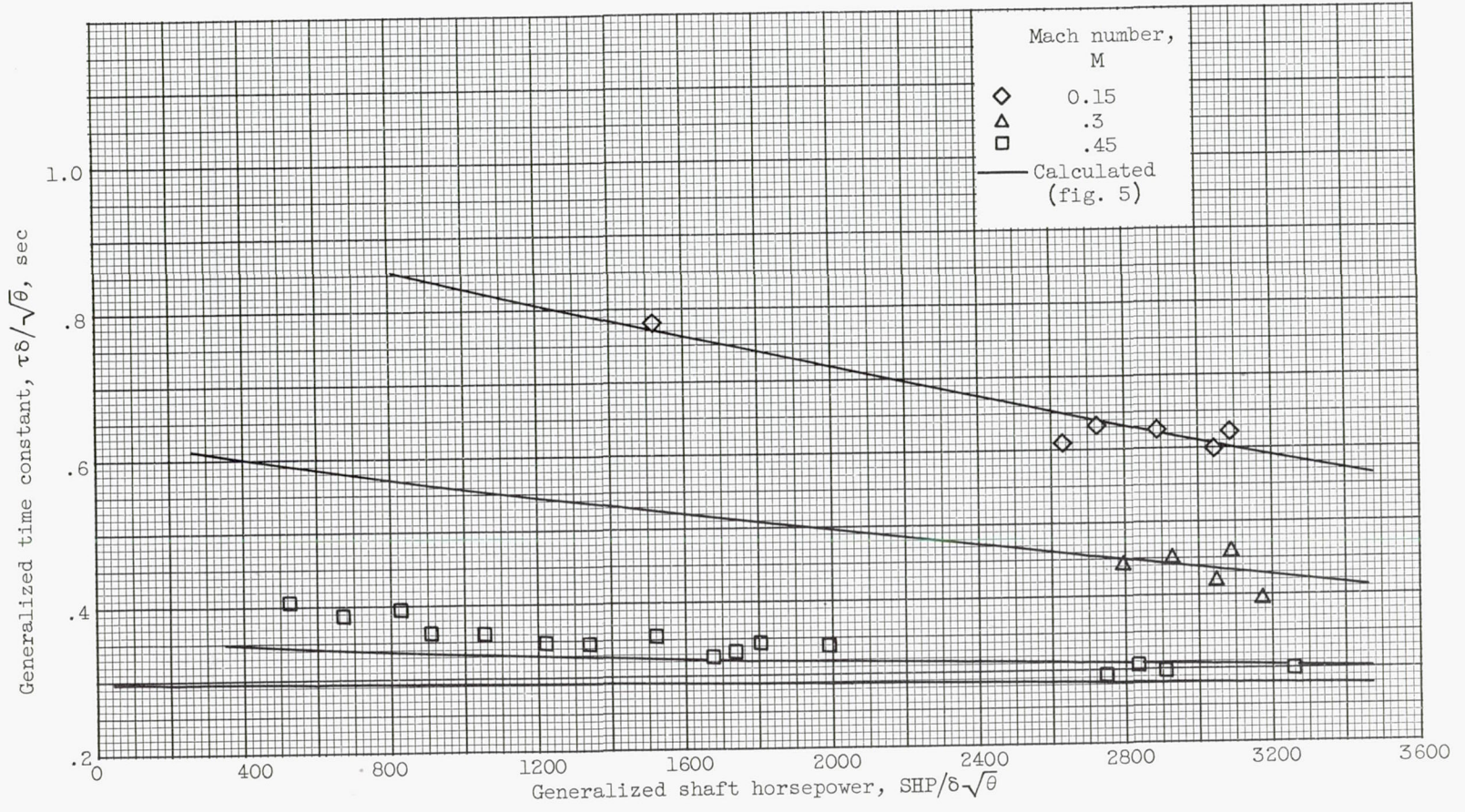   change in rotational speed.

Figure 10. - Comparison of time constant obtained by harmonic analysis of blade-angle steps with those calculated from steady-state characteristics.

(a) Fuel flow.

(b) Blade angle.

(c) Torque.

(d) Engine speed.

(e) Turbine-inlet temperature.

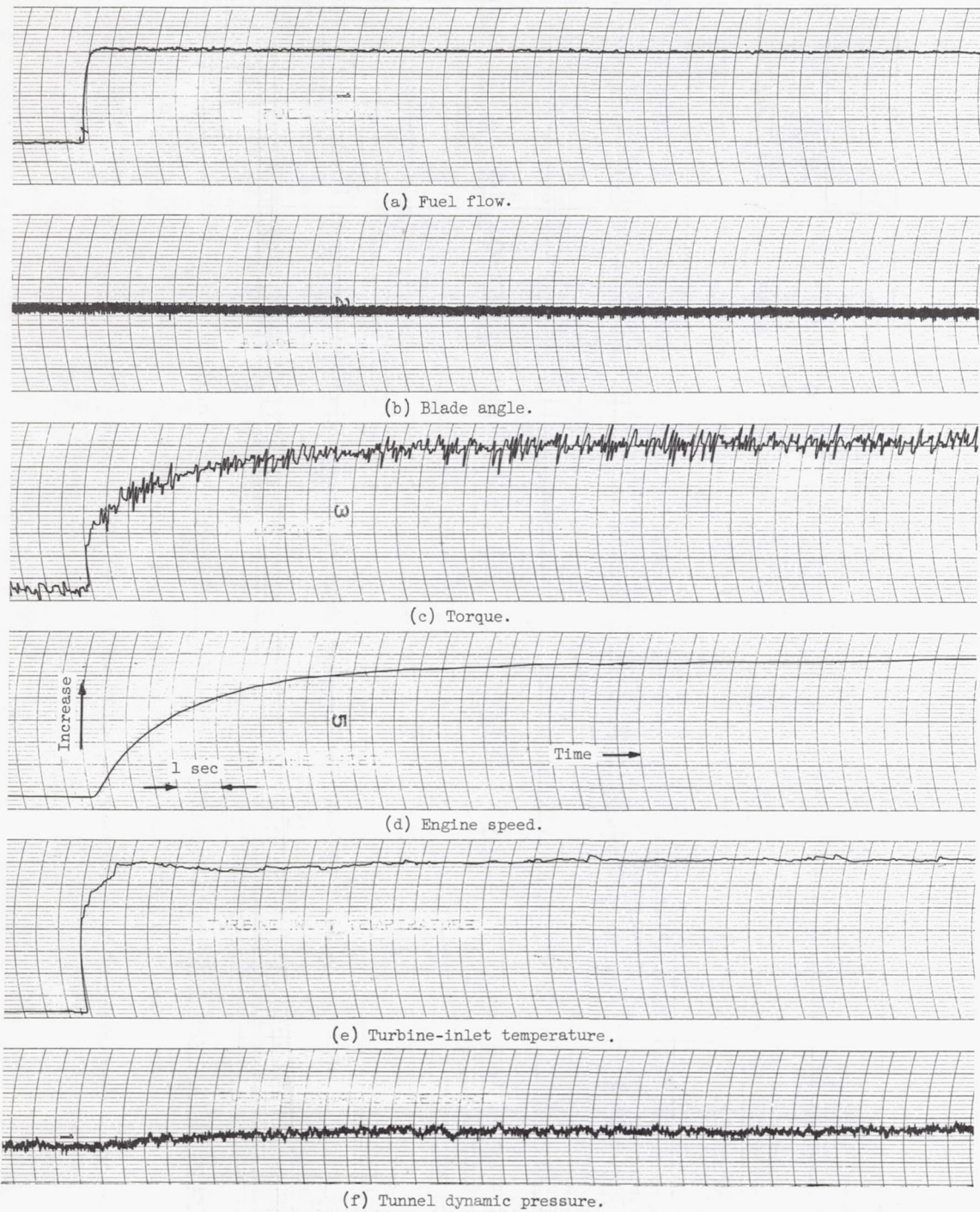(f) Tunnel dynamic pressure.

Figure 11. - Transient response of engine to fuel-flow step disturbance. Altitude, 35,000 feet;
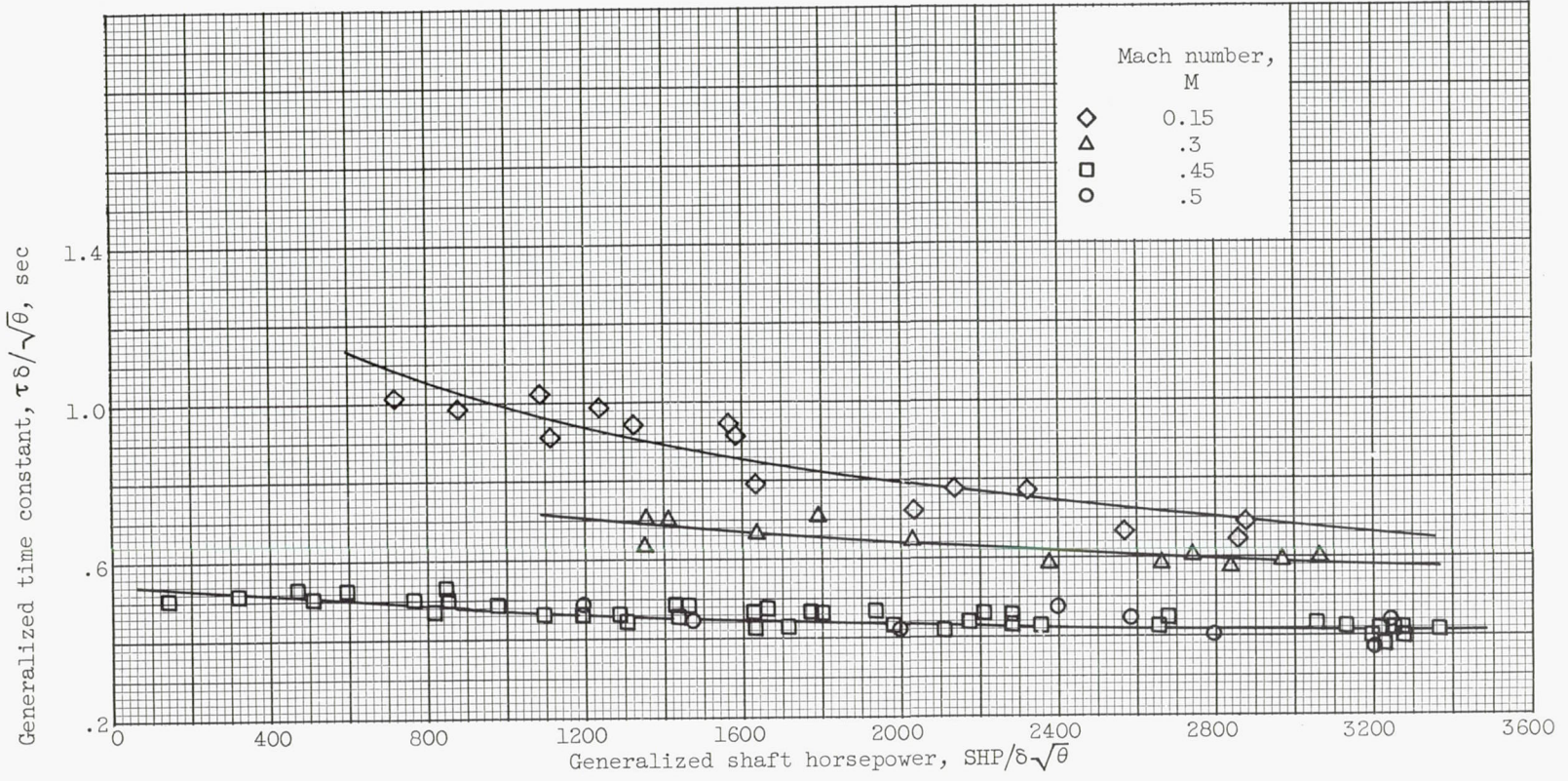Mach number, 0.45.

Figure 12. - Variation of generalized time constant with shaft horsepower. Altitude, 35,000 feet; fuel-flow step.